REPORT DOCUMENTATION PAGE

Form Approved OMB No. 0704-0188

Public reporting burden for this collection of information is estimated to average 1 hour per response, including the time for reviewing instructions, searching existing data sources, gathering and maintaining the data needed, and completing and reviewing the collection of information. Send comments regarding this burden estimate or any other aspect of this collection of information, including suggestions for reducing this burden to Washington Headquarters Services, Directorate for Information Operations and Reports, 1215 Jefferson Davis Highway, Suite 1204, Arlington, VA 22202-4302, and to the Office of Management and Budget, Paperwork Reduction Project (0704-0188), Washington, DC 20503.

1. AGENCY USE ONLY (Leave blank)	2. REPORT DATE 9 June 2000	3. REPORT TYPE AND DATES COVERED Final Report

4. TITLE AND SUBTITLE

High Average Power Solid-State Laser With Dynamic Self-Adaptive Cavity

5. FUNDING NUMBERS

F61775-99-WE

6. AUTHOR(S)

Dr. Oleg Antipov

7. PERFORMING ORGANIZATION NAME(S) AND ADDRESS(ES)

Institute of Applied Physics of the RAS
46 Uljanov Str.,
Nizhny Novgorod 603600
Russia

8. PERFORMING ORGANIZATION REPORT NUMBER

N/A

9. SPONSORING/MONITORING AGENCY NAME(S) AND ADDRESS(ES)

EOARD
PSC 802 BOX 14
FPO 09499-0200

10. SPONSORING/MONITORING AGENCY REPORT NUMBER

SPC 99-4028

11. SUPPLEMENTARY NOTES

12a. DISTRIBUTION/AVAILABILITY STATEMENT

Approved for public release; distribution is unlimited.

12b. DISTRIBUTION CODE

A

13. ABSTRACT (Maximum 200 words)

This report results from a contract tasking Institute of Applied Physics of the RAS as follows: The contractor will investigate the applicability of using a self-adaptive cavity for generation of Nd:YAG laser beams with average power approaching 500W and with near-diffraction limited spatial quality and good pointing stability.

14. SUBJECT TERMS

EOARD, Self-adaptive laser cavity, Solid state lasers, Laser beam control

15. NUMBER OF PAGES
24

16. PRICE CODE
N/A

17. SECURITY CLASSIFICATION OF REPORT UNCLASSIFIED	18. SECURITY CLASSIFICATION OF THIS PAGE UNCLASSIFIED	19, SECURITY CLASSIFICATION OF ABSTRACT UNCLASSIFIED	20. LIMITATION OF ABSTRACT UL

NSN 7540-01-280-5500

Standard Form 298 (Rev. 2-89)
Prescribed by ANSI Std. 239-18
298-102

Title of the Project: **High average power solid-state laser with dynamic self-adaptive cavity.**

The Final First-Year Report To European Office of Aerospace Research and Development (EOARD)

Name of Organization: Institute of Applied Physics (IAP) of the Russian Academy of Science (RAS).
Principal Investigator: Oleg Antipov
    Full home address: 7«A» boulevard Zarechniy, apartment 12, Nizhny Novgorod, 603032 Russia; home telephone: +7(8312) 192642.
    Office address: 46 Uljanov St., Nizhny Novgorod, 603600 Russia, IAP RAS; office telephone: +7(8312) 384547; fax: +7(8312) 363792.
    E-mail: antipov@appl.sci-nnov.ru

Date of completion: June 9, 2000

20000628 103

AGF 00-09-2894

TABLE OF CONTENTS

PAGE

1. LIST OF ABBREVIATIONS

LaC - Laser crystal;
SA   - Saturated absorber;
PG   - Population grating;
GG   - Gain grating;
RIG - Refractive index grating;
FWM - Four-wave mixing;
NDFWM- Nondegenerate four-wave mixing;
PC   - Phase conjugation;
DE   - Diffraction efficiency;
NLC - Nematic liquid crystal;

2. State-of-the-art of project implementation

During the fourth quarter of the project we continued our research in the following four main directions:

1. improvement of the theoretical model and continuation of numerical calculations of a self-starting Nd:YAG laser oscillator with a dynamic loop cavity completed by refractive index gratings (RIG's) and gain gratings (GG's) which accompany population gratings (PG's) induced inside the laser crystal (LaC) by generating beams themselves;

2. experimental investigations of the optimal scheme of the self-starting Nd:YAG laser oscillator with the dynamic cavity undertaken with the aim to increase the average power of a beam with near-diffraction limited quality;

3. experimental investigations of the laser based on another LaC (Nd:YAP) and Nd-containing laser glass with cavity formed with participation of RIG's and GG's inside the LaC or an absorption grating inside a saturated absorber (SA);

4. selection and purchase of optical elements and laser head components (laser crystals, head reflectors, flash lamps, etc.) which will be used in the high average-power laser with near diffraction limited beam quality.

All this activity is a continuation of the investigations started in the previous quarters of the project [1-4].

2.1. Numerical calculations

2.1.1. Set of equations

During the fourth quarter of the project we continued the numerical calculation of the self-starting laser oscillator with a cavity completed by RIG's and GG's accompanying PG's induced by generating beams in the amplifying LaC's. In comparison with previously reported results of numerical calculations [3,4], we assumed the presence of several longitudinal optical modes in the cavity with a nonlinear mirror. The mode conditions in the self-starting laser were achieved due to the requirement of phase synchronism of the initial wave and the nonlinearly reflected (phase-conjugate) wave. Each mode had its own spontaneous emission noise source (the random spatio-temporal delta-correlated function in the equations for optical wave amplitudes), however, additional noise PG's were assumed to be absent.

The idea of the last calculated multimode model is as follows. The interference fields of different optical modes are able to induce PG's with different spatial period. The optical wave can effectively reflect not only from the RIG's accompanying the PG's induced by this mode itself but also from RIG's induced by other modes with close wavelengths. In other words, modes with close wavelengths can induce approximately similar PG's. By this way, the different modes can interact one with another, providing generation conditions for the most effective mode. The concurrent-winner mode with maximum increment will generate in the self-starting laser.

In our calculations the plane generated waves intersecting at a small angle ($\Theta \ll 1$) in the LaC were assumed. We considered also that the interaction region of the optical waves is bounded by the area of optical pumping which was assumed to be rectangular. Using these considerations the equations for the optical waves were averaged in the transverse plane.

The calculated set of equations (for electrical fields of the m-th optical mode, $E_i^{(m)}$) was as follows.

$$\mu \frac{\partial E_1^{(m)}}{\partial t} + \frac{\partial E_1^{(m)}}{\partial z} = (\sigma_1^{(m)} N_0 + i\beta_2 M_0) E_1^{(m)} +$$

$$+ E_2^{(m)} \times \sum_{n=-Q}^{Q} [(\sigma_1^{(n)} N_{12}^{(n)} + i\beta_2 M_{12}^{(n)}) \cdot \exp(2i\Delta\mu(m-n)z)] +$$

$$+ E_3^{(m)} \times \sum_{n=-Q}^{Q} [(\sigma_1^{(n)} N_{13}^{(n)} + i\beta_2 M_{13}^{(n)}) \cdot \frac{Sin(2\Delta\mu\Theta x_0(n-m))}{2\Delta\mu\Theta x_0(n-m)}] + , (1.1)$$

$$+ E_4^{(m)} \times \sum_{n=-Q}^{Q} [(\sigma_1^{(n)} N_{14}^{(n)} + i\beta_2 M_{14}^{(n)}) \cdot \exp(2i\Delta\mu(m-n)z)] +$$

$$+ \sigma_1^{(m)} N_0 F_1(z,t) \exp\left(2\pi i \varphi_1(z,t)\right);$$

$$\mu \frac{\partial E_2^{(m)}}{\partial t} - \frac{\partial E_2^{(m)}}{\partial z} = (\sigma_1^{(m)} N_0 + i\beta_2 M_0) E_2^{(m)} +$$

$$+ E_1^{(m)} \times \sum_{n=-Q}^{Q} [(\sigma_1^{(n)} N_{12}^{*(n)} + i\beta_2 M_{12}^{*(n)}) \cdot \exp(2i\Delta\mu(m-n)z)] +$$

$$+ E_3^{(m)} \times \sum_{n=-Q}^{Q} [(\sigma_1^{(n)} N_{23}^{(n)} + i\beta_2 M_{23}^{(n)}) \cdot \frac{Sin(2\Delta\mu\Theta x_0(n-m))}{2\Delta\mu\Theta x_0(n-m)}] + , (1.2)$$

$$+ E_4^{(m)} \times \sum_{n=-Q}^{Q} [(\sigma_1^{(n)} N_{13}^{(n)} + i\beta_2 M_{13}^{(n)}) \cdot \exp(2i\Delta\mu(m-n)z)] +$$

$$+ \sigma_1^{(m)} N_0 F_2(z,t) \exp\left(2\pi i \varphi_2(z,t)\right);$$

$$\mu \frac{\partial E_3^{(m)}}{\partial t} + \frac{\partial E_3^{(m)}}{\partial z} = (\sigma_1^{(m)} N_0 + i\beta_2 M_0) E_3^{(m)} +$$

$$+ E_1^{(m)} \times \sum_{n=-Q}^{Q} [(\sigma_1^{(n)} N_{13}^{*(n)} + i\beta_2 M_{13}^{*(n)}) \cdot \frac{Sin(2\Delta\mu\Theta x_0(n-m))}{2\Delta\mu\Theta x_0(n-m)}] +$$

$$+ E_2^{(m)} \times \sum_{n=-Q}^{Q} [(\sigma_1^{(n)} N_{23}^{*(n)} + i\beta_2 M_{23}^{*(n)}) \cdot \exp(2i\Delta\mu(m-n)z)] +$$

$$, (1.3)$$

$$+ E_4^{(m)} \times \sum_{n=-Q}^{Q} [(\sigma_1^{(n)} N_{12}^{(n)} + i\beta_2 M_{12}^{(n)}) \cdot \exp(2i\Delta\mu(m-n)z)] +$$

$$+ \sigma_1^{(m)} N_0 F_3(z,t) \exp\left(2\pi i \varphi_3(z,t)\right);$$

$$\mu \frac{\partial E_4^{(m)}}{\partial t} + \frac{\partial E_4^{(m)}}{\partial z} = (\sigma_1^{(m)} N_0 + i\beta_2 M_0) E_4^{(m)} +$$

$$+ E_1^{(m)} \times \sum_{n=-Q}^{Q} [(\sigma_1^{(n)} N_{14}^{*(n)} + i\beta_2 M_{14}^{*(n)}) \cdot \exp(2i\Delta\mu(m-n)z)] +$$

$$+ E_2^{(m)} \times \sum_{k=-Q}^{Q} [(\sigma_1^{(n)} N_{13}^{*(n)} + i\beta_2 M_{13}^{*(n)}) \cdot \frac{Sin(2\Delta\mu\Theta x_0(n-m))}{2\Delta\mu\Theta x_0(n-m)}] + , \quad (1.4)$$

$$+ E_3^{(m)} \times \sum_{k=-Q}^{Q} [(\sigma_1^{(n)} N_{12}^{*(n)} + i\beta_2 M_{12}^{*(n)}) \cdot \exp(2i\Delta\mu(m-n)z)] +$$

$$+ \sigma_1^{(m)} N_0 F_4(z,t) \exp(2\pi i \varphi_4(z,t)),$$

$$\frac{\partial N_0}{\partial t} + N_0 = N_p(t) - N_0 \sum_{i=1}^{4} \sum_{k=-Q}^{Q} \left[|E_i^{(k)}|^2 \cdot \left(1 + \frac{k^2\Delta^2}{\delta^2}\right)^{-1} \right]$$

$$\frac{\partial N_{12}^{(m)}}{\partial t} + N_{12}^{(m)} = -N_{12}^{(m)} \sum_{i=1}^{4} \sum_{k=-Q}^{Q} \left[|E_i^{(k)}|^2 \cdot \left(1 + \frac{k^2\Delta^2}{\delta^2}\right)^{-1} \right] - N_0 \left(E_1^{(m)} E_2^{*(m)} + E_3^{(m)} E_4^{*(m)}\right) \cdot \left(1 + \frac{k^2\Delta^2}{\delta^2}\right)^{-1}$$

$$\frac{\partial N_{13}^{(m)}}{\partial t} + N_{13}^{(m)} = -N_{13}^{(m)} \sum_{i=1}^{4} \sum_{k=-Q}^{Q} \left[|E_i^{(k)}|^2 \cdot \left(1 + \frac{k^2\Delta^2}{\delta^2}\right)^{-1} \right] - N_0 \left(E_1^{(m)} E_3^{*(m)} + E_2^{(m)} E_4^{*(m)}\right) \cdot \left(1 + \frac{k^2\Delta^2}{\delta^2}\right)^{-1} , \quad (1.5)$$

$$\frac{\partial N_{14}^{(m)}}{\partial t} + N_{14}^{(m)} = -N_{14}^{(m)} \sum_{i=1}^{4} \sum_{k=-Q}^{Q} \left[|E_i^{(k)}|^2 \cdot \left(1 + \frac{k^2\Delta^2}{\delta^2}\right)^{-1} \right] - N_0 E_1^{(m)} E_4^{*(m)} \cdot \left(1 + \frac{k^2\Delta^2}{\delta^2}\right)^{-1}$$

$$\frac{\partial N_{23}^{(m)}}{\partial t} + N_{23}^{(m)} = -N_{23}^{(m)} \sum_{i=1}^{4} \sum_{k=-Q}^{Q} \left[|E_i^{(k)}|^2 \cdot \left(1 + \frac{k^2\Delta^2}{\delta^2}\right)^{-1} \right] - N_0 E_2^{(m)} E_3^{*(m)} \cdot \left(1 + \frac{k^2\Delta^2}{\delta^2}\right)^{-1}$$

$$\frac{\partial M_0}{\partial t} + \frac{M_0}{T_2} = \frac{N_0}{T_2} N_p(t); \frac{\partial M_{12}^{(m)}}{\partial t} + \frac{M_{12}^{(m)}}{T_2} = \frac{N_{12}^{(m)}}{T_2} N_p(t); \frac{\partial M_{13}^{(m)}}{\partial t} + \frac{M_{13}^{(m)}}{T_2} = \frac{N_{13}^{(m)}}{T_2} N_p(t);$$

$$\frac{\partial M_{14}^{(m)}}{\partial t} + \frac{M_{14}^{(m)}}{T_2} = \frac{N_{14}^{(m)}}{T_2} N_p(t); \frac{\partial M_{23}^{(m)}}{\partial t} + \frac{M_{23}^{(m)}}{T_2} = \frac{N_{23}^{(m)}}{T_2} N_p(t); \qquad , \quad (1.6)$$

---

where μ is the walk-off time in LaC, $\mu = l/(c\, T_1)$, c is the light velocity in the rod; all distances, times and intensities are normalized to the rod length (l), longitudinal relaxation time of the working transition (T_1), and saturation intensity (I_s), respectively; $\sigma_1^{(m)} = \sigma_0^{(m)}(1+i\beta'_1)$, $\sigma_0^{(m)}$ is the cross section of the working transition at the frequency of the m-th mode; β'_1 is the ratio of the real part of resonant susceptibility to the imaginary part for the $^4F_{3/2}$ level, $\beta'_1 = 4\pi^2 F_L^2 \Delta p_n /(\sigma_0 n_0 \lambda)$; β_2 is the nonlinearity coefficient determined by the polarizability of the $^2F(2)_{5/2}$ level, $\beta_2 = 4\pi^2 F_L^2 \Delta p_m/(n_0\lambda) \equiv \sigma_0 \beta'_2$; $F_1(z,t),...F_4(z,t)$ are amplitudes of the distributed Langevin's noise sources for spontaneous polarization; $\varphi_1(z,t),... \varphi_4(z,t)$ are phases of the Langevin's noise sources ($F_i(z,t)$ and $\varphi_i(z,t)$ are random delta-correlated functions); Δ is the intermode frequency range multiplied by T_1; δ is the luminescence linewidth multiplied by T_1; Θ is the angle of wave intersection; x_0 is the transverse range of the interaction region; m, n and k are the numbers of modes; $2Q+1$ is the total number of calculated modes, $N_p(t) = (e^{-t/t_{off}})^2(1-e^{-t/t_{on}})^2$ is the pump-speed function ($t_{off} = 300\,\mu s$, $t_{on} = 200\,\mu s$); T_2 is the lifetime of the $^2F(2)_{5/2}$ level.

The right-hand side of Eqs. (1.1-1.4) assumed scattering of the optical waves on gratings formed by all optical modes; however, the exponential factors and the factors of «sin x/x» limit the number of interacting waves. The right-hand side of Eqs. (1.5) for population assumed the saturation of the luminescence line by all optical modes. Equations. (1.6) assumed the existence of the $^2(F2)_{5/2}$ level which played a very important role in the formation of RIG's [2-5].

The "zero" initial conditions for all optical waves and the population gratings were used. The boundary conditions assumed the reflection of optical waves from external "ordinary" mirrors in the cavity.

2.1.2. Single mode model

When m=0 and 2Q+1=1, the set of Eqs. (1.1-1.6) describes single-mode generation in the center of the luminescence line. The calculation of the single-mode model showed the existence of the self-starting generation if the intensity of the initial noise-source for the weakest optical wave ($I_n = |F_1|^2/I_s$) exceeded a threshold level (Fig. 1) which was dependent on the small-signal gain $\alpha = 2\,\sigma_l\,N_0$.
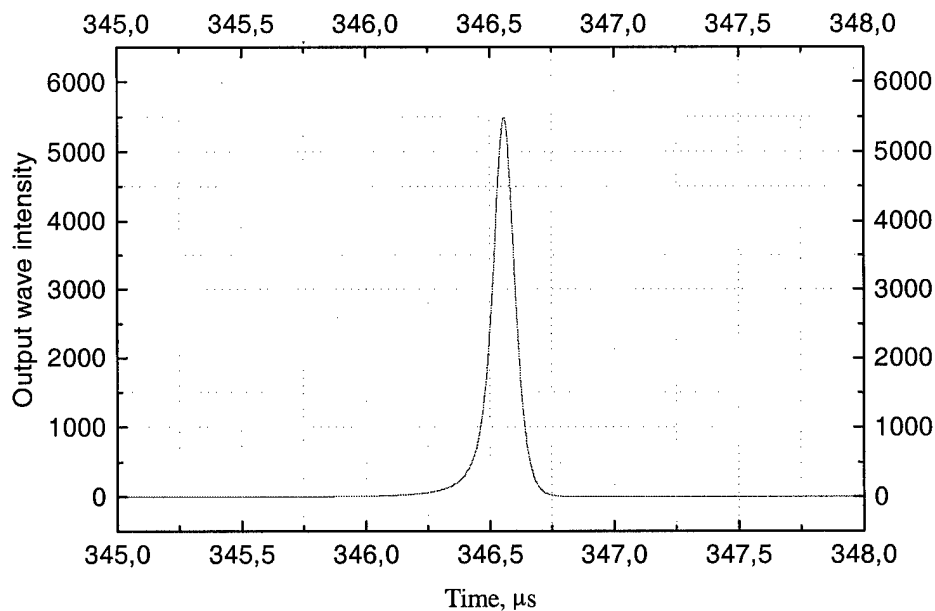

Fig. 1. Typical oscillogram of the output wave intensity in the model with one longitudinal mode (distributed delta-correlated noise source): for $\alpha l=4$ (equal to experimental threshold value), $\Omega T_1=5.5$, $I_n=1.5\bullet10^{-5}$ (near-threshold value). The pulse train consists of only one spike.

The existence of the self-starting oscillation in this model is in accordance with the results of previous calculations of the model with a boundary noise source for the weakest optical wave [1]. However, in the case of the distributed noise source the threshold for the initial noise was found to be much lower ($I_n\approx4\cdot10^{-8}$, at $\alpha l=4$) than for the boundary noise source ($I_n\approx1,5\cdot10^{-5}$) in the previous case.

It should be noted that in the distributed noise source model, when the initial noise is decreased to the threshold value, the generation domain on the scale of frequency detuning (ΩT_1) separates into numerous narrow lines with simultaneous narrowing of each line (Fig. 2). Within the common envelope the position of these lines, where generation is observed, is random, i.e., they are shifted from one calculation to another. Such behavior of the generation lines does not reflect, to our mind, any physical reality, but rather comes as a consequence of the mathematical model of stochastic noise source, which underlies the calculated equations. With increasing amplitude of the initial noise, these random lines of generation increase in number, and at a comparatively great initial noise ($I_n\approx2\cdot10^{-5}\cdot$) the generation domain becomes continuous. The width of this continuous generation band already reflects the regularity of the physical system which requires a certain synchronism of generation waves and provides different increments for different generation waves when they are nonlinearly reflected from RIG's.

6
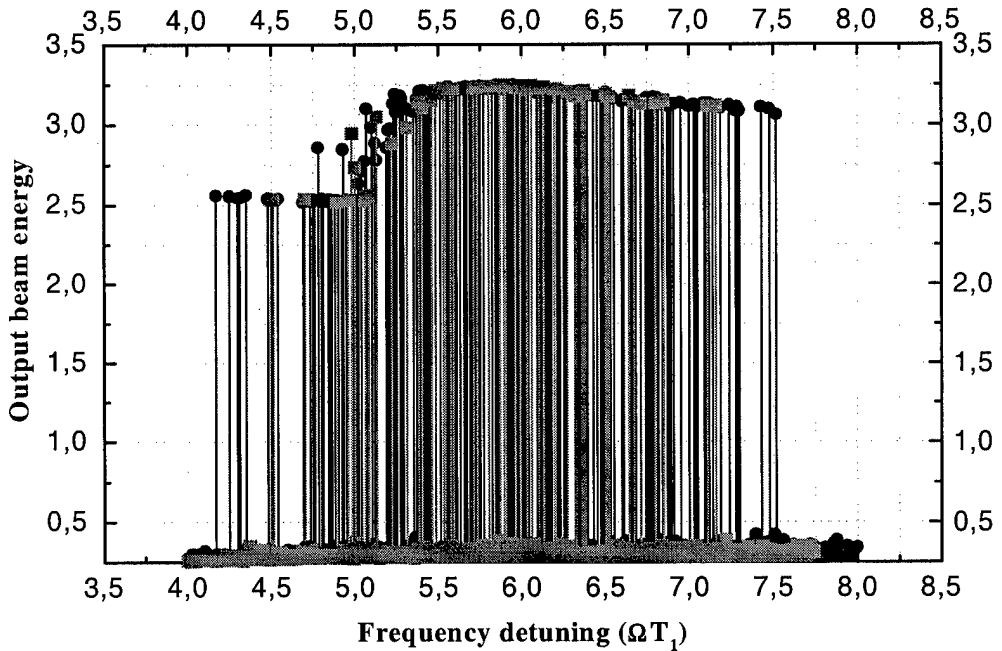
Fig. 2. Output wave energy vs intracavity frequency detuning for $\alpha l = 4$, $I_n = 1{,}525{\cdot}10^{-5}$ (blue curve) and $I_n = 1{,}5{\cdot}10^{-5}$ (red curve). Calculation was performed with ΩT_1-step of 0.01.

Although the single mode model is rather simple, it should be noted, however, that the intensity of threshold noise in our calculations appears to be quite high for the amplifier gain that corresponds to the experimentally observed threshold of generation ($I_n \approx 1.5 \times 10^{-5}$, at $\alpha l = 4$). The high level of the threshold noise is inconsistent with the theory of optical noise in laser amplifiers. Indeed, it is well known that the initial noise source for the optical wave in a real laser system can be estimated by the expression $I_n \approx \theta^2 \cdot \dfrac{\delta v}{\Delta v} \cdot I_{sat}$, where θ is the divergence of the optical beam, $\delta \omega$ is the frequency bandwidth of the generated pulse, and $\Delta \omega$ is the bandwidth of the luminescence line [6]. Under our experimental conditions, the optical beam divergence was about $\theta \approx 10^{-3}$, $(\delta \omega / \Delta \omega) \approx 10^{-3}$, and I_n is estimated to be about $\sim 10^{-9}\ I_{sat}$. However, calculations yield a comparable level of the initial noise only for the large gain ($\alpha l = 8$). This disagreement between the theory and experiments requires additional explanations which could be found by calculating a more complicated multimode model of the laser.

2.1.3. Multimode model

The intermode frequency spacing between longitudinal modes of the self-starting laser cavity is about $(2L)^{-1}$ [sm^{-1}] where L is the total length of the cavity. In our experiment L was $\sim$2-5 m. The great number of the longitudinal modes can be situated at frequencies within the luminescence line of Nd:YAG crystal with the width of $\Delta v \sim 6$ cm^{-1}. The luminescence noise in each mode can participate in the initial stage of grating formation even when the mode does not generate. In other words, several longitudinal modes can jointly induce the PG's accompanied by RIG's and GG's, providing the self-starting oscillation conditions.

A drawback of the joint grating formation is the wavelength difference that leads to phase mismatch in the gratings induced by different modes. This phase mismatch gives the exponential factors and the «sin x/x» factors in the grating terms of the right-hand side of Eqs. (1.1.)-(1.4.). If this phase mismatch along the interaction distance is much greater than 2π, the reflection of the waves on an alien grating is incoherent, and the reflected wave will not grow.

The small-scale transmitting gratings and the large-scale reflecting gratings have different spatio-temporal selectivity. The phase mismatches of the small-scale reflecting gratings induced by different optical longitudinal modes (at frequencies within the luminescent line) are determined by $\Delta k\, l \approx \Delta\lambda\, l\, /\, \lambda^2$. For a Nd:YAG rod with length of $l = 10$ cm, $\Delta k\, l \approx 2\pi$ if $\Delta v \sim 10^{-1}$ cm^{-1}, which is much less than

7

the total luminescence line. So, a small number of longitudinal modes can participate in the formation of the joint reflection grating.

The phase mismatch of the large-scale transmitting grating induced by waves with different wave vectors is determined by $\Delta k\, d_x\, sin\theta \approx \Delta\lambda\, /\lambda^2\, d_x\, sin\theta$. Under the ordinary conditions of our experiment $d_x \sim 5$ mm and $\theta \approx 0.1...0.01$, the great mismatch ($\sim 2\pi$) is realized only for $\Delta k \sim 20...200$ cm^{-1}, which is much more than the Nd:YAG luminescence line. So, this means that the different optical waves (the longitudinal modes) at frequencies within the total luminescence line can participate in the joint grating formation. If the shape of the luminescence line were rectangular, all modes would induce the transmitting PG with equal efficiency, and the self-starting condition of the laser would be described by the same set of equations as for the single mode which induced only the transmitting grating. In this case the effective intensity of the noise source can be estimated by the expression $I_n \approx \theta^2 \cdot I_{sat} \sim 10^{-6} I_{sat}$, and this level of the initial noise source is comparable with the results of calculations that predict the self-starting oscillations.

The specific role of the transmission grating in the process of cavity formation is confirmed by the results of our previous experiments. The scheme of the self-starting Nd:YAG laser with a large-scale transmission grating has demonstrated lower threshold of self-excitation than in the laser with a small-scale reflection grating [7].

The model with several longitudinal modes was calculated by using the set of Eqs. (1.1)-(1.6). Three or five longitudinal modes (one at the center of the luminescence line and two modes at the both sides from the center, Fig. 3) were taken into consideration.
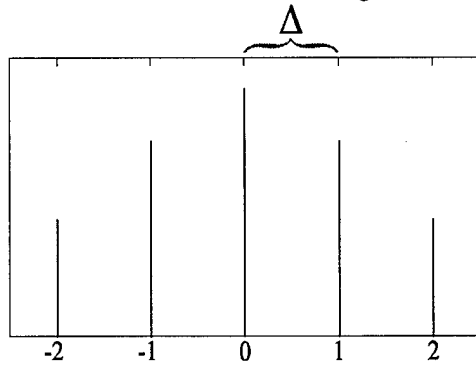
Fig. 3. Diagram of the initial intensity of luminescence components for 5 calculated modes near the center of the line ($v = 0$).

The calculations showed the existence of self-starting oscillations in the system for different frequency detuning at frequencies within the luminescence line (Δ-parameter was varied from 0.001 to 0.2).

It is very important that the generation of only the central mode was realized (Fig. 4). The predominance of the central mode can be explained by several factors: 1) the difference in the «linear» gain of the components; 2) the difference in the initial noise for luminescence components; 3) the difference in nonlinear amplification. The first two factors were the same as in the case of a linear laser. The latter factor takes place only for the self-starting laser with a nonlinear mirror. All these factors can explain the single-mode generation in the self-starting laser. The existence of the additional factor in the self-starting laser means that longitudinal modes are better discriminated in the nonlinear cavity than in the linear cavity.

In some realizations of calculations, a next-standing mode with the anti-Stokes frequency detuning generated with a delay from the central mode spike, but energy of the next-generated wave was always much less than energy of the central mode (Fig. 4).

8
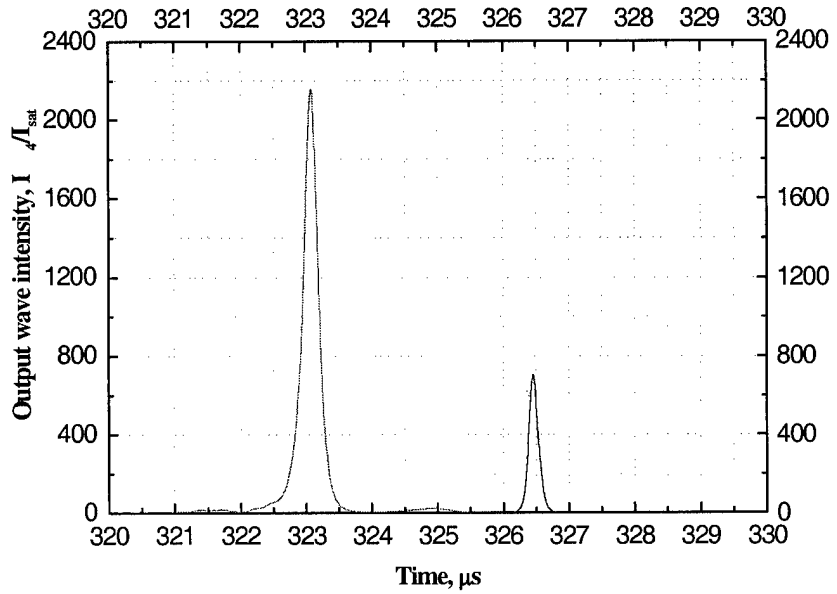
Fig. 4. Oscillogram of the output wave intensity in the model with
5 longitudinal modes: «0» (central) mode – red curve, «-1» mode
– blue curve. Parameters are: $\Omega T_1 = 4.7$, logarithmic gain $\alpha l = 4$, I_n
$= 1.6 \cdot 10^{-5}$, $\Delta = 0.01$.

One more consequence of the calculations is a decrease in the initial noise level for the central mode (
I_n) which is required for the self-starting generation (Fig. 5 and 6). The calculations show that the
threshold decreased with an increase in the number of modes taken into consideration.
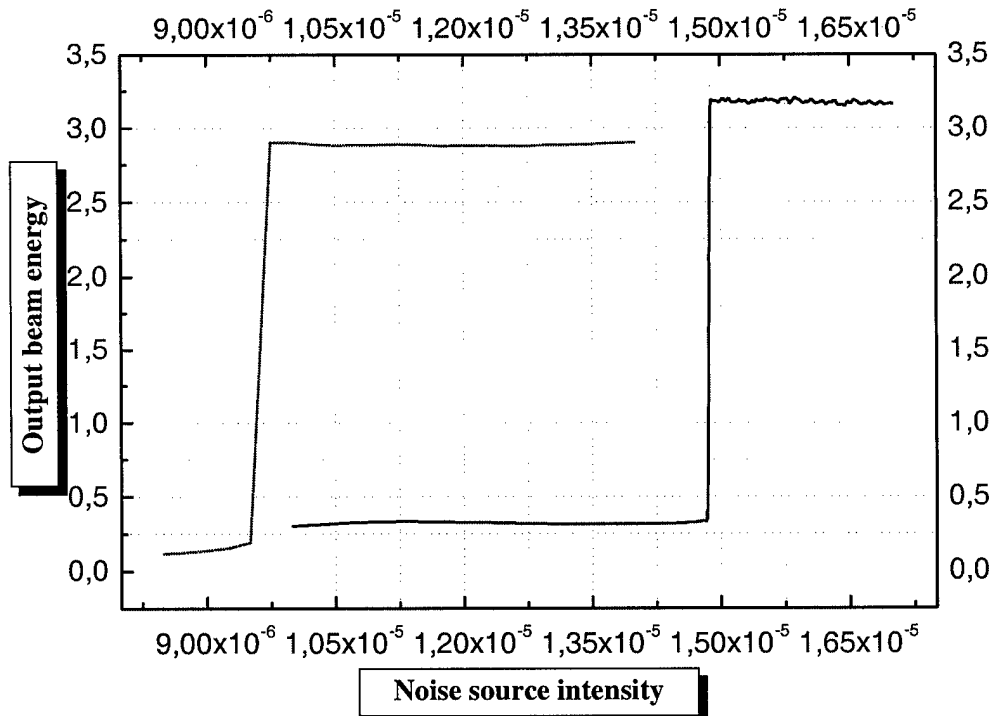
Fig. 5. Output beam energy vs noise source intensity for a model with 1 frequency mode (blue curve) and 3
modes ($\Delta = 0.01$, red curve). Logarithmic gain (intensity) $\alpha l = 4$, frequency detuning ΩT_1 is nearly optimal for
each curve.

9
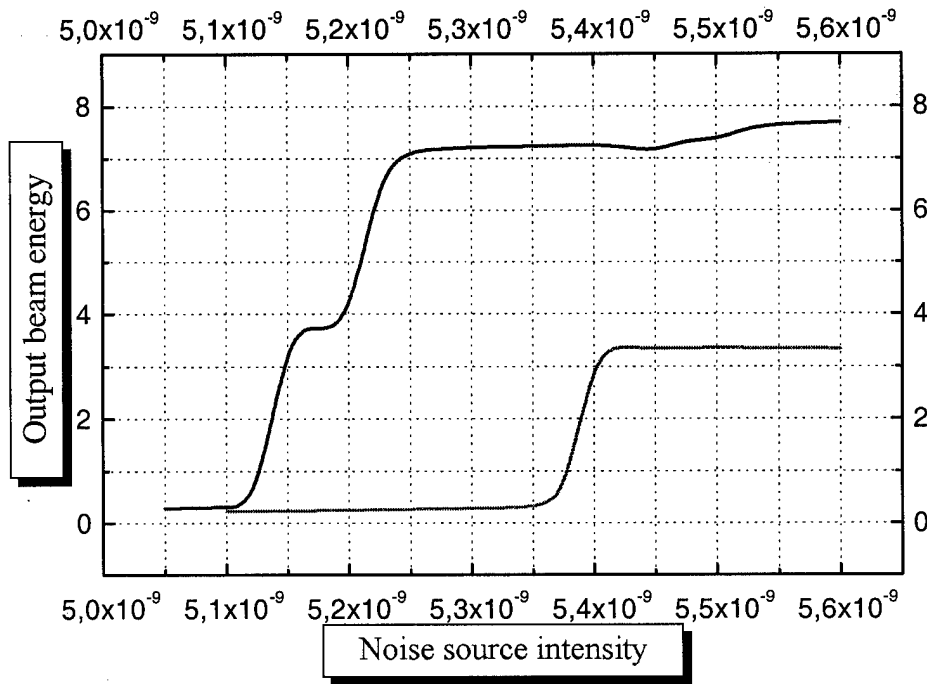
Fig. 6. Output beam energy vs noise source intensity for different numbers of modes: 1 mode (red curve) and 3 modes (Δ=0.1, blue curve). Logarithmic gain (intensity) αl=6, frequency detuning ΩT_1 is optimal for each curve.

Unfortunately, the calculations of each realization for the multimode model are time-consuming (even using modern computers with Pentium III processor). The calculations of the model with even 7-10 modes are hardly acceptable in practice. Therefore, the multimode noise could be taken into consideration by the noised PG's. This approach is similar to that reported previously in paper [4], where a strong decrease in threshold of the self-starting oscillation was shown.

Summarizing the results presented in this section, it should be noted that the multimode luminescence noise participates at the initial stage of formation of transmitting PG. Then the threshold of the self-starting oscillation is determined by the total intensity of luminescence of the Nd:YAG crystal due to joint formation of large-scale transmission gratings.

2.1.4. The role of diffuse reflection at the boundary and noise scattering inside the crystal

One more cause of the decrease in threshold of self-starting oscillations is the diffuse reflection at the LaC's boundary. We analyzed the diffuse reflection on the LaC boundary using the boundary condition at the output end of the LaC:

$$E_1(0,t) = \sqrt{R} \cdot (E_2(0,t) + E_4(0,t)),$$

where R is the reflection coefficient.

The calculation showed a decrease in the threshold noise intensity with increasing reflection coefficient (see Fig. 7, where R=1 corresponds to threshold of the linear generation).
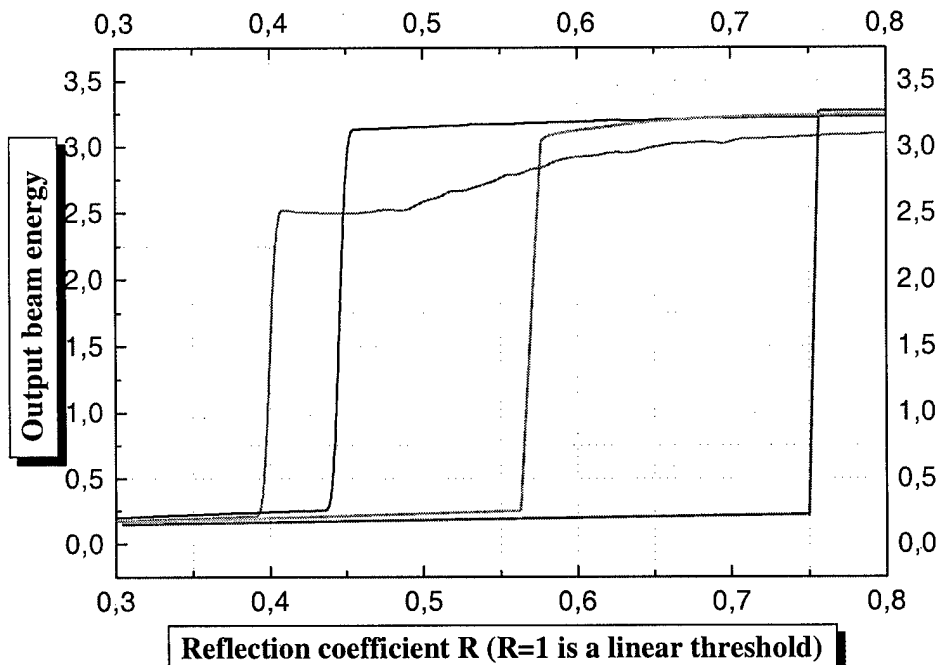
Fig. 7. Output beam energy vs reflection coefficient R of the output boundary for different noise source intensities: $I_n \approx 10^{-7}$ (red curve), $I_n \approx 10^{-9}$ (blue curve), $I_n \approx 10^{-10}$ (pink curve), and $I_n \approx 10^{-11}$ (green curve).

Scattering from occasional inhomogeneities and defects inside a crystal plays the same role. To analyze this factor, we calculated a set of Eqs. (1.1)-(1.6) by determining additional noised RIG's. The calculations showed a decrease in threshold of the spontaneous noise intensity (I_n) with increasing noise-grating amplitude.

The diffuse scattering at boundaries of optical elements and scattering from occasional inhomogeneities and defects can strongly decrease the threshold of the nonlinear oscillation in the laser. This fact appears to be trivial if we will take into account that the occasional scattering and reflection increase the intensity of optical waves in the nonlinear laser medium, and the field of interference of these waves will induce the nonlinear grating, providing self-starting conditions.

It should be noted that threshold gain for the «nonlinear» generation was found to be less than the linear generation threshold. This means that even if the threshold of the linear generation could be exceeded (due to occasional scattering or diffuse reflection) and at slow pump increasing, the "nonlinear" generation starts earlier than the "linear" generation. However, if the "linear" reflection coefficient is much greater than the "nonlinear" reflection from the dynamic grating, the mode formation will be determined by the linear cavity.

2.2. Experimental study of the laser on population gratings

Our pervious study of the loop scheme has shown the possibility of generation of 200W-average-power beams with near-diffraction quality [4]. The experiments performed during this phase of the project were directed at

1. the investigation of ways to increase the output power of generating beam in a scheme comprising amplifiers with larger Nd:YAG rods ($\varnothing$10 mm×135 mm);
   - adding one more pass of the generated beam through an amplifier;
   - using mirrors with curvature;
   - using an intracavity phase plate;
2. the investigation of the possibility to use other active media (Nd:YAP crystal and Nd:glass) in the self-starting laser architecture.

2.2.1. The scheme comprising two amplifiers with large Nd:YAG rods

The possibility of increasing the average power of the generated beams with a good quality with larger Nd:YAG rods of $\varnothing 10$ mm$\times$135 mm in amplifiers by use of one more pass of generated beam through the amplifier was investigated. We used laser rods with the concentration of Nd^{3+} ions of about 1.1% and standard quality. The laser rods were produced in Laser Material Corporation (USA).
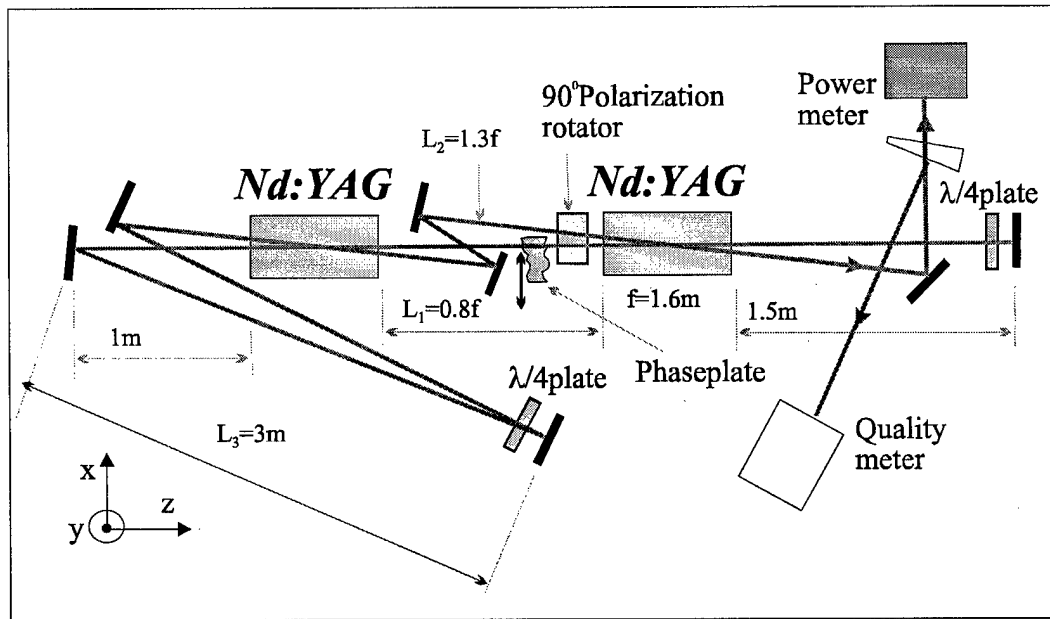

Fig. 8. The experimental setup of self-starting scheme based on two amplifiers (Nd:YAG rods with sizes $\varnothing 10\times 135$ mm).

The scheme comprising two amplifiers with these Nd:YAG rods was studied (Fig. 8). The amplifiers provided double flash lamp pumping to each rod with maximum pump pulse energy up to 200 J at a repetition rate of 30 Hz. The strong thermal lenses were induced in laser crystals under this pumping. The focal distances of the lenses depended on pump pulse energy, repetition rate and temperature of cooling water. The influence of the focal distances on optimal distances between the amplifiers and mirrors required to achieve maximum output beam power and good quality was investigated. It was found that an increase in the focal distances by 1.5 times (due to improved cooling) leads to a necessity to have the same increase in the distances between the amplifiers and mirrors in order to achieve the same average power of the beam and its quality (Fig. 9). The normalized distances between the amplifiers and mirrors determined from the focal distance of a lens thermally induced in the amplifiers are shown in Fig. 8.

To decrease polarization distortions, we used a $\lambda/4$ plate and a quartz polarization rotator. These elements allowed for rotation of the generated wave polarization by 90^0 after passage through each amplifier. Therefore the polarization distortions appearing during one passage through the amplifier were compensated during the next passage. This method for compensating polarization distortions has been used in construction of solid-state lasers [9]. It can be seen that the average power of the generation beam did not depend on the presence of polarization elements. At the same time, the beam quality strongly depended on the pump power, the presence of polarization elements, and the scheme length.
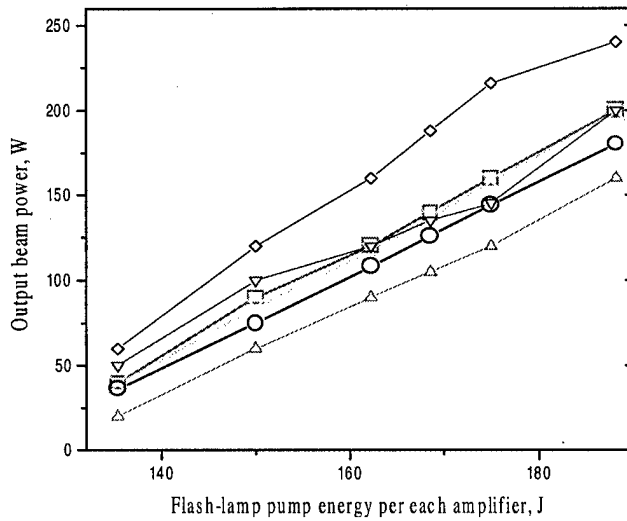
Fig. 9. Average power of the generated beam as a function of pump pulse energy of each amplifier in the scheme with two Nd:YAG amplifiers (circles – scheme of Fig. 8 without polarization elements with L_3=0, crosses – scheme of Fig. 8 without polarization elements, with L_3=3 m and without phase plate, squares – scheme of Fig. 8 with polarization elements, with L_3=3 m and without phase plate, down-triangles - scheme of Fig. 10 with plane mirror and polarization elements, diamonds - scheme of Fig. 10 comprising a mirror with curvature and polarization elements, up-triangles - scheme of Fig. 8 with polarization elements, with L_3=3 m and with phase plate). The repetition rate is 30 Hz.
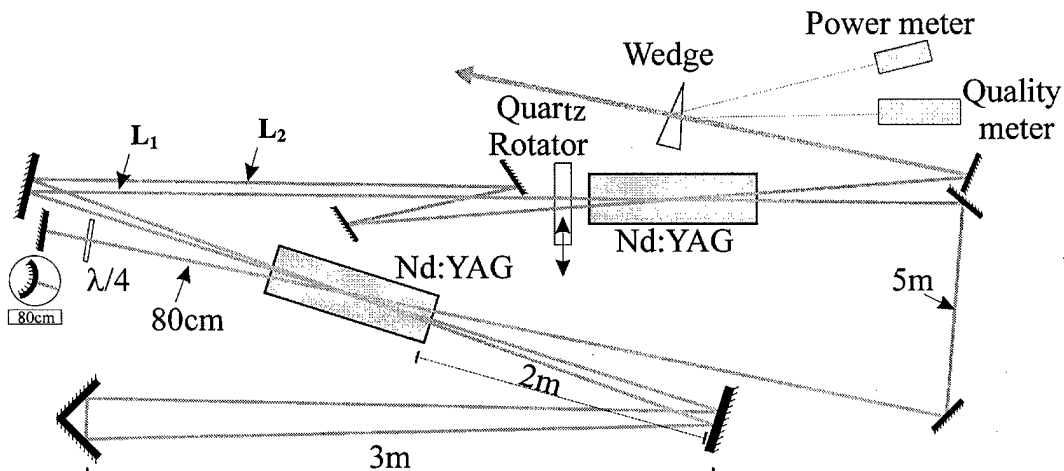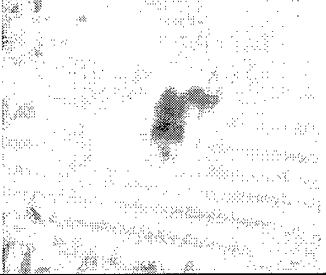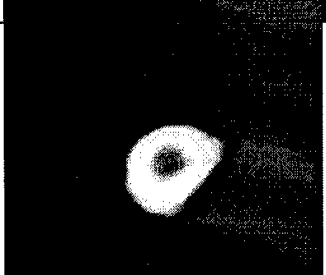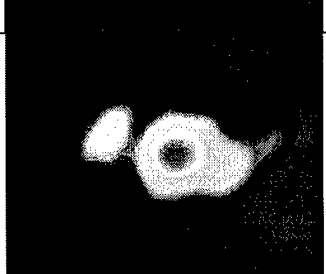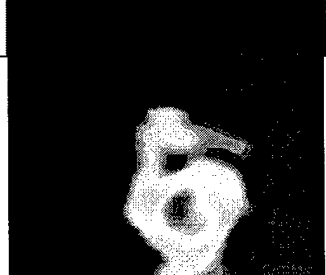

Fig. 10. The experimental setup of the self-starting scheme with two amplifiers (Nd:YAG rods ∅10×135 mm) with an additional pass of the generated beam through one amplifier. Two variants of the scheme: with a plane mirror and a mirror with the curvature radius of 80 cm.

It has been previously observed (see 4-report, [4]) that the average power of the generated beam achieves 200 W (corresponding to a pulse energy of 6.7 J) (Fig. 9). The possibility of increasing the output power of the generating beam by adding one more pass of the generated beam through an amplifier was investigated (Fig. 10). It was found that in this case the average power of the output beam did not change (Fig. 9). However, the quality of the beam worsened, the M^2 parameter was 2.6 in the x direction and 3.1 in the y direction. An increase in the average power of the output beam was observed when a mirror with curvature was used to compensate thermal focusing in the additional pass (Fig. 10). The average power achieved 240 W (Fig. 9), but the quality of the beam decreased, the M^2 parameter was 3.5 in the x direction and 2.7 in the y direction. The results are summarized in Table 1.

13

Table 1.

Scheme	Maximum average power achieved	$M^2_{x,y}$-parameter at maximal power	Beam profile in focal plane of the lens
Fig.8 L1=1.3 m L2=2.1 m L3=0 Without polarisation rotation	180 W	$M^2_x=11$ $M^2_y=14$	
Fig.8 L1=1.3 m L2=2.1 m L3=3 m Without polarisation rotation	200 W	$M^2_x=5.1$ $M^2_y=4.4$	
Fig.8 L1=1.3 m L2=2.1 m L3=3 m With polarisation rotation	200 W	$M^2_x=1.7$ $M^2_y=2.2$	
Fig.10 L1=1.3 m L2=2.1 m With polarisation rotation, with plane mirror.	200 W	$M^2_x=2.6$ $M^2_y=3.1$	
Fig.10 L1=1.3 m L2=2.1 m With polarisation rotation, with mirror having curvature.	250 W	$M^2_x=3.5$ $M^2_y=2.7$	
Fig.8 L1=1.3 m L2=2.1 m L3=4 m With polarisation rotation, with phase plate	160 W	$M^2_x=1.5$ $M^2_y=3.6$	

It can be seen that best results were observed in the scheme (Fig. 8) with large lengths and polarization rotation elements. The profiles of the beam in the near and far field generated in the optimal scheme with and without phase plate are shown in Fig. 11. The average power of the generation beam in the near field was 200 W. The transformation of the output beam profile during its propagation was studied. The average power of the beam core inside $\varnothing$13 mm in the far field was 100W. The difference is caused by large-angle components, and the power of the core indicates the ability of the generated beam to provide large-distance energy transfer.

The deviations in the generation direction were observed at maximum pump power (at pump pulse energy of 200 J for each amplifier and a repetition rate of 30 Hz). These deviations led to movement of the beam in the far field. The range of this movement coincided with the diameter of the generated beam's core. It was found that these deviations were caused by instability of the pulse energy of flash-lamp pumping (due to the instability of power supply), which led to an instability of the focal distance of thermal lenses and instability of thermal edges induced in amplifiers. The deviations were minimized at a lower repetition rate when power supply of the amplifiers worked in a mode that provided high stability of pump pulse energy. At a repetition rate of 22 Hz and the same pump pulse energy the beam's shift in the far field was less than 20% of the beam diameter, however the average power of the generated beam decreased by 25% in this case.


a)   b)
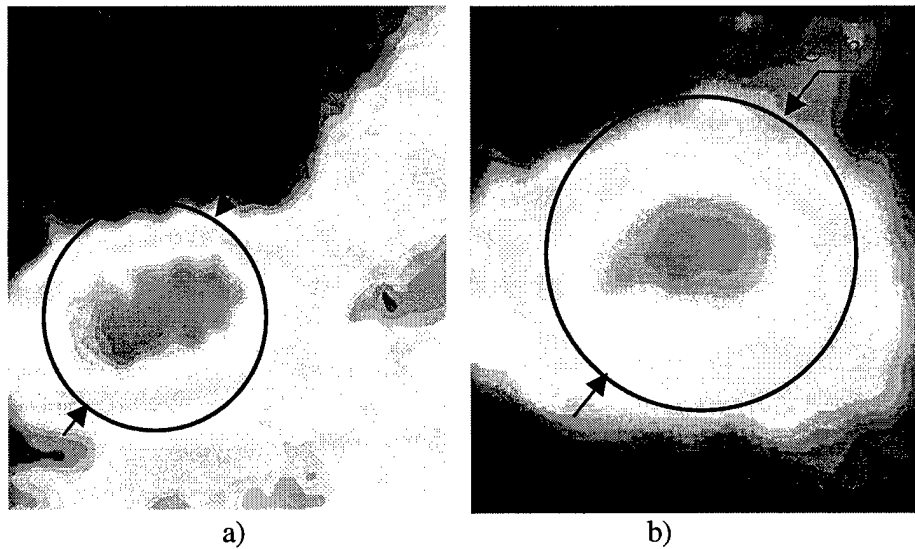
Fig. 11. Transverse profiles of the generation beam at distances 3 m (a) and 17 m (b) from the output of the laser.

The self-adaptive properties of the scheme were tested by inserting a phase plate with large aberrations (it increased the divergence of a beam by 10 times) (Fig. 8). It was observed that the average power of the generated beam decreased to 160 W. The quality of the beam remained near diffraction (M^2_x=1.5, M^2_y=3.6). This result showed the self-adaptability of the nonlinear dynamic cavity to phase distortions. The mechanism for this adaptability is shown in Fig. 12. The nonlinear holographic cavity is formed so that the output beam E_4 and the initial noise E_1 are near Gaussian and are close to phase conjugated beams which play a role of pumping waves in the four-wave interaction. The beam E_2 , which is strongly aberrated, interacts with the pumping waves in the Nd:YAG amplifier. This four-wave interaction gives rise to a beam E_3 that is phase conjugated to E_2. Thus all phase distortions that deteriorated the beam E_2 are compensated for the beam E_3. The near-Gaussian beam E_3' has small aperture losses in the long-distance scheme and transforms to a near-Gaussian output beam E_4. In order to decrease the generation threshold and therefore increase the generated pulse energy, the beam E_2 is reflected backward by the mirror. This provides a high initial level for the conjugated beam E_3. Indeed, the linear reflection of the beam E_2 has a component that is phase conjugated. At the same time, a non-conjugated component will be deteriorated once again by the

15

phase plate and will have very large losses in the long-distance scheme with Fresnel parameter of 1-3. Therefore we provide conditions under which the self-starting scheme is forced to operate in the phase conjugation mode with a near-Gaussian output beam.

The profiles of the beam in the near and far fields generated in the optimal scheme with a phase plate are shown in Fig. 13. The average power of the generation beam in the near field was 160 W. The transformation of the output beam profile during its propagation was studied. The average power of the beam core inside $\varnothing$ 17 mm in the far field was 75W. It can be seen that the contributions to the large-angle components and to the central core are approximately the same as in the scheme without phase plate. This demonstrates one more time the ability of the dynamic cavity to compensate internal phase distortions.
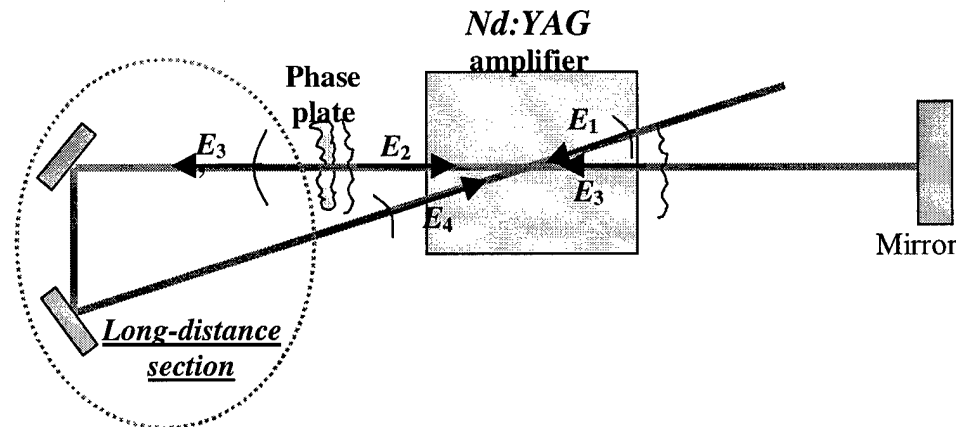
Fig. 12. Schematic view of four-wave mixing in self-starting laser-oscillator that provides self-adaptive compensation for phase distortions.
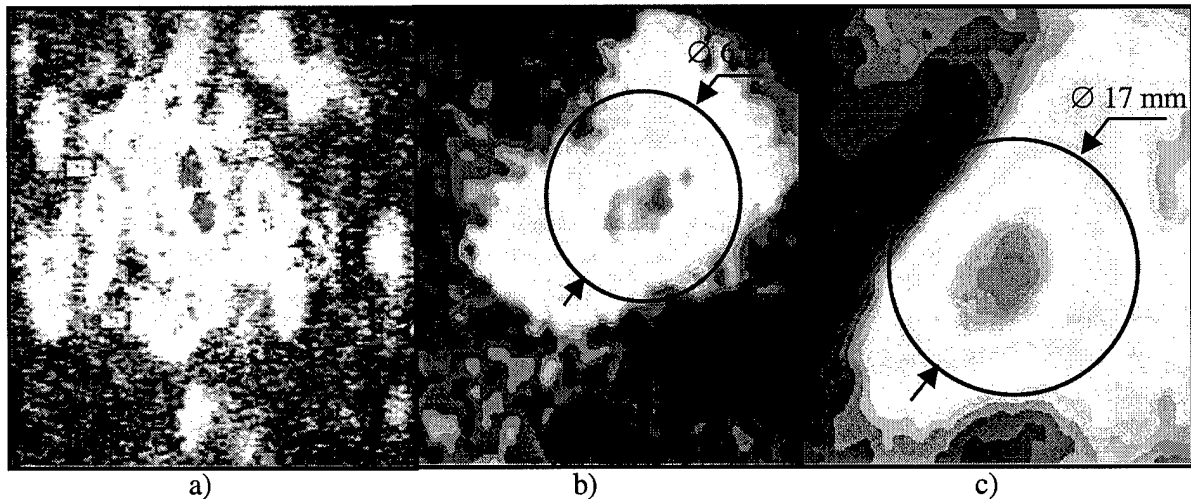
Fig. 13. Transverse profile of a Gaussian beam passed through the phase plate in the far field (a). Transverse profiles of the generation beam at distances 3 m (b) and 17 m (c) from the output of the laser with a phase plate.

Thus the self-adaptive properties of nonlinear holographic mirror were shown. Having the scheme incorporating a phase plate with high aberrations as an example, we demonstrated how aberrations thermally induced in laser crystals are compensated by a nonlinear holographic cavity. The conditions for generation of a beam with high quality and high average power were determined. It was demonstrated that beam distortions caused by the birefringence thermally induced in a Nd:YAG rod can be significantly reduced by using polarization rotation elements. A further increase in the average power and quality of the generated beam can be achieved by use of diode pumping.

16

2.2.2. Search for new materials for self-starting laser oscillator.

The possibility of using another active medium, a $Nd:YAlO_3$ crystal (Nd:YAP), in the self-starting laser architecture was investigated. This laser medium has higher saturation intensity in comparison with Nd:YAG. However, its thermo-physical characteristics are worse than those of Nd:YAG, which results in greater thermo-induced phase distortions.

The standard scheme of the self-starting «single-loop» laser was studied. It was found that the self-starting generation can be realized in a laser oscillator comprising two Nd:YAP crystals 6 mm in diameter and 100 mm in length. The average power of the self-starting generation achieved 48 W at pump pulse energy 63 J for each crystal and repetition rate of 30 Hz. The M^2 parameter of the generated beam was about 4.6, which is worse than in a similar scheme based on Nd:YAG crystals.

The possibility of using Nd-containing silicate laser glass («GLS-6» type, according to russian specification) in the self-starting laser architecture was investigated. We used one- and two-loop geometry of the self-starting laser based on one Nd:glass rod 12 mm in diameter and 260 mm in length. It was observed that the self-starting generation could not be realized at pump pulse energy up to 1700 J and repetition rate 0.1 Hz.

2.3. References

1. The first report to EOARD for the project *"High average power solid-state laser with dynamic self-adaptive cavity"*, presented to EOARD at June 24, 1999.
2. The second report to EOARD for the project *"High average power solid-state laser with dynamic self-adaptive cavity"*, presented to EOARD at August 13, 1999.
3. The third report to EOARD for the project *"High average power solid-state laser with dynamic self-adaptive cavity"*, presented to EOARD at November 14, 1999.
4. The forth report to EOARD for the project *"High average power solid-state laser with dynamic self-adaptive cavity"*, presented to EOARD at February 18, 2000.
5. O.L. Antipov, A.S. Kuzhelev, D.V. Chausov, A.P. Zinov'ev, *"Dynamics of refractive index changes in Nd:YAG laser crystal under Nd^{3+}-ions excitation"*, J. Opt. Soc. of America B **16**, 1072-1079 (1999).
6. G.J. Linford, E.R. Peressini, W.R. Sooy, M.L. Spaer, *"Very long lasers"*, Applied Optics **13**, 379-390 (1974).
7. O.L. Antipov, A.S. Kuzhelev, A.P. Zinov'ev, "High average-power solid-state lasers with cavity formed by self-induced refractive index gratings," in Laser resonators II, A.V. Kudryashov and P. Galarneau, eds., Proc. SPIE **3611**, 147-156 (1999).

2.4. Selection and purchase of the optical elements and laser head components

During the fourth quarter of the project we have purchased one more Nd:YAG rod with larger diameter, 12 mm, and with length 135 mm, from US "Laser Material Corporation".

We suppose to purchase laser diode arrays with cw power at 40-60W for pumping of Nd:YAG amplifiers. The possible producer is Semiconductor Laser International Corporation (15 Link Drive Binghamton, NY 13904, tel: (607)7223800, fax: (607)7223900, e-mail: sli@slicorp.com, www.slicorp.com).

3. Technical description of the first-year achievements

3.1. Summarized results of numerical calculations

- **Models of the system.**

The self-starting oscillations in the laser system with «linear» and «loop» feedback were studied numerically by using the plane-wave approximation. The existence of RIG's and GG's that accompany PG's in a Nd:YAG amplifier was assumed. The RIG was supposed to be caused by different polarisability of excited and unexcited Nd^{3+} ions and to be mainly connected with the population (or depopulation) of the higher lying energy level $^2(F2)_{5/2}$. The dynamics of this level was taken into account.

Several models of temporal structures of the optical beam were used:
- monochromatic waves;
- several monochromatic components within the Nd:YAG luminescence band (3 or 5 components);
- monochromatic waves + broadband noised waves;
- multimode optical waves at frequencies within the luminescence band.

The Langevin-noise sources for spontaneous emission and noised PG's were used in numerical analysis of the self-starting conditions.

The role of scattering on occasional inhomogeneities and LaC defects, and of diffuse reflection from the rod's end was also studied.

- **The self-starting conditions.**

All models used have demonstrated the possibility of self-starting oscillations (in the «linear» generation) when amplifier gain achieved a threshold level. It was found that another critical parameter for the self-starting generation is the amplitude of noise sources for the spontaneous emission or random PG's. The threshold value of the noise-source amplitude depends on the amplifier gain and the model of optical beam and noise used.

In the model of monochromatic optical waves, the calculated threshold level for the noise-source amplitude of the spontaneous emission was found to be several orders of magnitude higher than it could be possible in experiment. Further investigations showed that all monochromatic optical waves initiated by spontaneous emission within the whole luminescence line take part in the formation of the common large-scale transmission PG at the pre-generation stage. So, the initial large-scale PG is formed by the total spontaneous emission within the Nd:YAG luminescence line of the working transition.

The threshold of the self-starting oscillation decreases in the presence of noised PG's or spontaneous scattering on micro-irregularities of LaC's or diffuse scattering on the rod end. All these factors help the self-oscillations to start. In all cases, the threshold of nonlinear oscillation was found to be less than the threshold of «linear» generation (due to the «linear» noised feedback).

- **The nonlinear stage of generation.**

The generated beam intensity and the generated-pulse energy increase almost linearly with increasing unsaturated amplifier gain. It was found that the generated intensity (or energy) is almost independent of the initial noise level.

The single-longitudinal mode regime of the generation was calculated even in the presence of several noised optical components. It was determined that longitudinal modes are well discriminated in the laser with a nonlinear mirror (better than in the laser with linear mirrors). The predomination of the mode in the center of the luminescence line is caused not only by maximum «linear» gain (similarly as in an ordinary laser) but also maximum nonlinear energy transfer (and nonlinear positive feedback) by the induced dynamic RIG's and GG's.

- **The model of the self-starting laser with cavity completed by dynamic RIG inside NLC.**

The cavity of the self-starting laser can be completed by dynamic RIG's induced by generated beams inside the NLC layer with thermal or orientational nonlinearity. The dynamical behavior of the laser was found to be similar to that of the laser based on PG's inside LaC's. The generated-pulse energy in

18

the laser is determined by unsaturated gain in laser amplifiers and nonlinear coefficient of the NLC layer.

3.2. Summarized main experimental results.

- During the period of project implementation we have determined how to realize a self-starting laser with high average power of generated beams (up to 200 W) and near-diffraction beam quality (with M^2 parameter less than 2).
  1. The amplifiers should be located so that their thermally induced lenses form a telescopic system. In other words, they should be placed at a distance equal to about two focal distances of the thermal lenses. Other distances between amplifiers and mirrors where the beam is collimated should be large enough to provide the total Fresnel number close to unity ($N=1$-3).

Indeed, when thermal lenses form a telescopic system the generated beam has maximum diameter in both amplifiers. So, the generated beam gets much energy stored in the amplifiers. On the other hand, the generated beam has smaller aperture losses between the amplifiers and mirrors if the beam is collimated. These distances should be very large to provide the selection of a Gaussian mode (the total Fresnel number $N=1$-3), so for a beam with large divergence the aperture losses will dramatically increase. The telescopic system provides the collimation and hence low losses for the Gaussian mode.

  2. The distortions of the generated beam caused by thermally induced birefringence can be reduced by use of polarization rotation elements (a quartz rotator and a $\lambda/4$ plate).

These elements should be located so as to provide the rotation of the generated wave polarization by 90^0 after passage through each amplifier. Therefore polarization distortions that occur during one passage through the amplifier will be compensated during the next passage. This method for compensating polarization distortions has been used in construction of solid-state lasers [9]. In our experiments, the average power of the generation beam did not depend on the presence of polarization elements. At the same time, the beam quality strongly depended on their presence.

  3. The role of a Sagnac interferometer in selective properties of the self-starting laser cavity was investigated. We found that the use of Sagnac interferometer in the cavity does not provide for any additional selection of spatial modes, as expected previously.

We compared two identical schemes with and without Sagnac interferometer. The same average power of the generated beam was realized when a Sagnac interferometer was replaced by an ordinary mirror positioned at a definite distance from the amplifier. The quality of the output beam was the same in the both cases.

  4. The quality of the generated beam can be increased by use of a saturable absorber $LiF:F_2^-$. In this case, there was a slight reduction in the average power of the output beam (by 10-20%). The duration of the generated pulses in the train decreased from 300-500 ns to 50-150 ns by incorporating the SA into the scheme.

The possibility of using saturable absorbers $LiF:F_2^-$ and $Cr^{4+}:YAG$ to shorten the generated pulses was investigated. We varied the location of the absorbers, its transparency and type. It was found that most preferable for such self-starting laser is a $LiF:F_2^-$ absorber with a transparency of 40-60%. It provided pulse shortening to durations of 100-150 ns. Its optimal location in the scheme is in the area of beam intersection between the amplifiers. In this position additional gratings are written in the SA by generated beams, which increases the efficiency of distributed feedback. The SA also plays a role of a soft diaphragm. There is a focal plane of the thermal lenses in the area of beam intersection between amplifiers. That is why a soft diaphragm (in the SA) in this area decreases the divergence of the generated beam and improves its quality.

  5. The optimal duration of the pump pulses is 0.3 ms. The small-signal amplification at each amplifier should achieve 100 to significantly exceed the generation threshold.

An increase in the generated beam power was observed when pulse duration increased from 0.2 ms to 0.3 ms. This result can be explained by that the amplitude of the RIG caused by the population of the high lying level $^2F(2)_{5/2}$ depends on the simultaneous presence of the flash-lamp pumping and the population of the metastable level $^4F_{3/2}$. Thus the amplitude of the RIG increases at increasing pump pulse duration. A further increase in the pump pulse duration (more than 300-400 μs) led to a decrease

in the average power of the output beam. This can be due to a decrease in amplification and pump power, which took place when the pump duration increased at a constant pump-pulse energy. This decrease had two results: first, movement toward generation threshold and, second, a decrease in the amplitude of the RIG (the amplitude of the RIG caused by population of the high lying level $^{2}F2_{5/2}$ depends strongly on the amplification and pump power). It was determined that the optimal pump pulse duration for the two-Nd:YAG-amplifier scheme is about 0.3 ms.

- The formation of refractive-index gratings, their dynamics and origin were investigated by use of the nondegenerate four-wave mixing (NDFWM) technique. It was confirmed that the cavity is formed by refractive-index gratings accompanying population gratings written in the laser crystal by generating beams themselves.

The dynamic cavity of the laser oscillator was formed with participation of PG's written in Nd:YAG crystals by generation beams themselves. The PG's were accompanied both by the gain and refractive-index gratings. Our theoretical estimations and numerical calculations have shown the important role of the RIG's that provide the positive distributed feedback in the cavity. In this experiment we verified the hypothesis about the existence and importance of the RIG's completing the cavity. To achieve this, we used the NDFWM technique.

The intersecting waves of generation induce PG's in the Nd:YAG amplifier. The large-scale RIG accompanying the PG was read by an optical wave of a Q-switched Nd:phosphate-glass laser with another wavelength of 1054 nm. Using this NDFWM method we separated the resonantly induced RIG from the GG's in inverted Nd:YAG. The propagation direction of the reading beam was chosen as optimal for Brag diffraction on the recorded grating and was nearly backward to the direction of one writing generation beam, so that wave synchronism took place.

The pulse of the testing laser beam with duration of 160 ns was synchronized with some variable delay at the beginning of the generation pulse. By changing this delay time we can study temporal dynamics of the tested grating. The measured diffraction efficiency (DE) of the RIG, defined as the ratio of energies of the diffracted beam and the reading beam at 1054 nm, depended on the delay of the reading beam pulse at the onset of generation. The investigation on the fast time scale showed that the DE of the resonant RIG began to increase several microseconds before the generation onset. The formation of the nonlinear RIG mirror that completes the cavity preceded the first optical generation spike. The DE strongly increased (more than by an order of magnitude) after the beginning of the laser generation and decreased after its end.

The DE at the time of generation onset was about $5 \cdot 10^{-7}$. Using this value of the nonlinear mirror «reflectivity» we estimated the threshold gain of the amplifiers in the self-starting generator. For generation to start in the cavity completed by the RIG, the total amplification should be greater than the total losses which are caused mostly by the RIG reflectivity. In this case the amplification of each Nd:YAG amplifier (K) at generation threshold must be $K_{th} \approx \left(5 \cdot 10^{-7}\right)^{-0.25} = 44.7$. This estimation of K_{th} is in good accord with experimental measurements of the gain of the Nd:YAG amplifiers at the generation threshold (see Fig. 11a). Therefore it is possible to draw a conclusion that the generation in the investigated loop scheme is indeed caused by the self-consistent processes of RIG formation and the increase in the amplitude of the generated waves reflected from the RIG.

- The possibility of using another nonlinear medium for grating's formation (nematic liquid crystals (NLC) with orientational and thermal nonlinearity) was investigated.

The study of a laser with a dynamic cavity completed by RIGs induced in an NLC by generating waves was aimed at understanding the general principles of operation of the self-starting laser with a nonlinear mirror.

It is known that liquid crystals have extraordinarily large slow-response nonlinearities, such as orientational and thermal. These nonlinearities allow to realize effective degenerate two-wave and four-wave mixings of the optical beams. Therefore, the use of the NLCs in the self-starting lasers for the formation of nonlinear mirrors is particularly attractive for the quasi-cw generation with high beam quality. On the other hand, the inertial nonlinearity of NLC seems to be quite similar to the resonant

nonlinear changes of refractive index of the laser crystals (such as Nd:YAG). For this reason, the study of the self-starting laser based on the NLC cell offers a good opportunity for understanding the general principles of completing a laser cavity by slow-response RIG in self-starting lasers.

The experimental system of the laser oscillator consisted of three flash-lamp-pumped Nd:YAG amplifiers with rods 100 mm in length and 6.3 mm in diameter, a polarizer, «linear» mirrors, and a NLC cell. This arrangement provided four-wave interactions of the self-intersecting generated beam which started from spontaneous emission.

We used NLC cells with different thickness of nematic materials. The nonlinear generation was realized by orientational nonlinearity in a 75μm layer of pure 5CB (with the temperature of nematic-isotropic transition of 36^0C) with planar orientation of the NLC director. The nonlinear generation caused by thermal nonlinearity was realized with a 0.5 mm layer of pure 5CB with the homeotropic orientation of the NLC director induced by the dc electric field applied to the walls and a 5 mm layer of cianobephenils mixture with the transition temperature of 59^0C and the electrically induced homeotropic orientation.

The experiments with high repetition rate showed good direction stability and high quality of the output beam in the schemes with all cells. The pulse shape was temporary smooth, the single-longitudinal mode generation with good quality of the beam was observed. However, the average power of the generated beam was only up to several watts.

Thus the principles of cavity formation in self-starting laser-oscillator by RIG's were verified at the example of a laser with the nonlinear holographic mirror induced in NLC.

- The possibility to utilize another laser medium (Nd:YAP crystals and Nd:Glass) was investigated. It was found that the Nd:YAG crystal is the best candidate to be used as a laser medium and as a medium for grating formation.

The Nd:YAP crystal is a laser medium that possesses higher saturation intensity in comparison with Nd:YAG. However, its thermo-physical characteristics are worse than those of Nd:YAG, which results in greater thermally induced phase distortions.

It was found that the self-starting generation could be realized in a laser oscillator comprising two Nd:YAP crystals. The average power of the self-starting generation achieved 48 W and the M^2 parameter of the generated beam was about 4.6, which is worse than in a similar scheme based on Nd:YAG crystals.

Our study of the possibility to use Nd:glass in the self-starting laser architecture showed that the self-starting generation cannot be realized at a pump pulse energy up to 1700 J.

- The self-adaptive properties of the scheme were tested by introducing a phase plate with large aberrations (which increased the divergence of a beam by 10 times) into the scheme. The average power and quality of the output beam did not change significantly (no more than by 20%). This result demonstrates the self-adaptive properties of the nonlinear dynamic cavity to phase distortions.

The main point of our investigation is to create a self-adaptive laser system that provides generation of high average power beam with near-diffraction quality. It was shown that under conditions of strong thermal aberrations and lensing in Nd:YAG amplifiers the self-starting laser generates a beam with an average power of up to 200 W with quality parameter M^2=1.5-2. This result indicates the adaptability of the nonlinear cavity to thermal aberrations. Discussing the scheme with a phase plate with high aberrations as an example, we demonstrated how aberrations thermally induced in the laser crystals are compensated by nonlinear holographic cavity.

4. Presentations of the results

4.1. Published papers.

1. O.L. Antipov, A.S. Kuzhelev, D.V. Chausov, A.P. Zinov'ev, A.V. Fedin, A.V. Gavrilov, S.N. Smetanin, "100W-average-power Nd:YAG laser with adaptive cavity formed by self-induced population gratings," Abstract of a report for the Advanced High-Power Laser and Application Conference (ALPHA'2000, 1-5 November, 1999, Osaka, Japan), paper 3889-88.

2. A.S. Kuzhelev, O.L. Antipov, D.V. Chausov, A.P. Zinov'ev, "Dynamics of high-average-power Nd:YAG lasers with distributed feedback by self-induced population gratings," Summary for the International Conference for Student, Young Specialists and Engineers «Optics'99» (19-21 October 1999, St. Petersburg, Russia), pp. 96-97 (1999).

3. O.L. Antipov, A.S. Kuzhelev, D.V. Chausov, A.P. Zinov'ev, A.V. Fedin, A.V. Gavrilov, S.N. Smetanin, "100W-average-power Nd:YAG laser with adaptive cavity formed by self-induced population gratings," Advanced High-Power Laser and Application Conference (ALPHA'2000, 1-5 November, 1999, Osaka, Japan), Proceeding of SPIE V. 3889, paper 3889-88 (1999).

4. O.L. Antipov, A.S. Kuzhelev, D.V. Chausov "Formation of the dynamic cavity completed by resonant refractive index gratings in a self-starting high-average-power Nd:YAG laser-oscillator," Optics Express, v. 5, N12, pp.286-292 (1999).

5. O.L. Antipov, A.S. Kuzhelev, A.P. Zinov'ev, O.N. Eremeykin, "Self-starting laser with a nonlinear liquid crystal mirror," Nonlinear Materials, Devices and Applications, part of SPIE's Symposium on High-Power Lasers and Application, 22-28 Jan 2000, San Jose, CA, USA, SPIE Proceeding, V. 3928, paper 3928-21 (2000).

6. O.L. Antipov, A.S. Kuzhelev, D.V. Chausov, A.P. Zinov'ev, O.N. Eremeykin, A.V. Fedin, A.V. Gavrilov, S.N. Smetanin, "Self-starting 100W-average-power laser with a self-adaptive cavity", Laser Resonators III, part of SPIE's Symposium on High-Power Lasers and Application, 22-28 Jan 2000, San Jose, CA, USA, SPIE Proceeding, V. 3930, paper 3930-15 (2000).

7. A.S. Kuzhelev, O.L. Antipov, D.V. Chausov, "Resonant refractive index grating as a self-adaptive mirror for high-average-power Nd:YAG laser" Technical digest of Conference on Lasers and Electro-Optics, (7-12 May, 2000, San Francisco, California, USA), paper CMH6, pp. 42-43 (2000).

8. A.S. Kuzhelev, A.P. Zinov'ev, O.N. Eremeykin, O.L. Antipov, R. Macdonald, " Self-starting laser with cavity completed by dynamic holographic grating induced in a nematic liquid crystal near phase transition point" Technical digest of Conference on Lasers and Electro-Optics, (7-12 May, 2000, San Francisco, California,USA), paper CMH7, pp. 43-44 (2000).

9. O.L. Antipov, A.S. Kuzhelev, D.V. Chausov, A.P. Zinov'ev, "Nd:YAG laser with self-adaptive cavity completed by dynamic resonant refractive-index gratings," Technical Digest of the 10th Conference on Laser Optics (June 26-30, 2000, St. Petersburg, Russia) Invited paper ThC1-21.

4.2. Presentations in the Conferences.

1. Conference "Advanced High-Power Laser and Application" (ALPHA'2000, 1-5 November, Osaka, Japan), O.L. Antipov, A.S. Kuzhelev, D.V. Chausov, A.P. Zinov'ev, A.V. Fedin, A.V. Gavrilov, S.N. Smetanin, "100W-average-power Nd:YAG laser with adaptive cavity formed by self-induced population gratings," poster presentation 3889-88.

2. International Conference for Student, Young Specialists and Engineers «Optics'99» (19-21 October 1999, St. Petersburg, Russia), A.S. Kuzhelev, O.L. Antipov, D.V. Chausov, A.P. Zinov'ev, "Dynamics of high-average-power Nd:YAG lasers with distributed feedback by self-induced population gratings", Oral presentation, presented by Dr. A.S. Kuzhelev.

3. Conference "Photonics West'2000" (22-28 Jan 2000, San Jose, CA, USA), Laser Resonators III, part of SPIE's Symposium on High-Power Lasers and Application, O.L. Antipov, A.S. Kuzhelev, D.V. Chausov, A.P. Zinoviev, O.N. Eremeykin, A.V. Fedin, A.V. Gavrilov, S.N. Smetanin, "Self-starting 100W-average-power laser with a self-adaptive cavity". Oral presentation 3930-15, presented by Dr. O.L. Antipov.

22

4. International Conference "Photonics West'2000" (22-28 Jan. 2000, San Jose, CA, USA), subconference Nonlinear Materials, Devices and Applications, part of SPIE's Symposium on High-Power Lasers and Application, O.L. Antipov, A.S. Kuzhelev, A.P. Zinov'ev, O.N. Eremeykin, "Self-starting laser with a nonlinear liquid crystal mirror," Oral presentation 3928-21, presented by Dr. O.L. Antipov.
5. Conference on Lasers and Electro-Optics, (7-12 May, 2000, San Francisco, California,USA), A.S. Kuzhelev, O.L. Antipov, D.V. Chausov, "Resonant refractive index grating as a self-adaptive mirror for high-average-power Nd:YAG laser" Oral presentation CMH6, presented by Dr. A.S. Kuzhelev.
6. Conference on Lasers and Electro-Optics, (7-12 May, 2000, San Francisco, California,USA), A.S. Kuzhelev, A.P. Zinov'ev, O.N. Eremeykin, O.L. Antipov, R. Macdonald, " Self-starting laser with cavity completed by dynamic holographic grating induced in a nematic liquid crystal near phase transition point" Oral presentation CMH7, presented by Dr. A.S. Kuzhelev.
7. The 10th Conference on Laser Optics (June 26-30, 2000, St. Petersburg, Russia) O.L. Antipov, A.S. Kuzhelev, D.V. Chausov, A.P. Zinov'ev, "Nd:YAG laser with self-adaptive cavity completed by dynamic resonant refractive-index gratings," Invited paper ThC1-21, will be presented by Dr. O.L. Antipov.

5. Directions of further investigations

The experimental investigation of self-starting oscillators should be continued in the following directions:

1. An additional increase in output power (up to 0.4-0.5 kW) of the self-starting laser system based on the flash-lamp pumped Nd:YAG crystals could be achieved by increasing the active volume:
- using larger sizes of Nd:YAG rods (reasonable diameter of the amplifier could be up to 12..13 mm at the concentration of Nd^{3+} ions of about 1%);
- using an additional (third) laser amplifier with a Nd:YAG rod of large diameter.
2. It seems to be very attractive to study the possibility of using the diode-pumped LaC's for creation of a self-starting laser system with the reciprocal cavity (as a competitive approach to the nonreciprocal self-starting laser system presented recently by Dr. M.J. Damzen at CLEO'2000, [M. Trew, G..J. Crofts, M.J. Damzen et al., «Multi-watt continuous-wave diode-pumped $Nd:YVO_4$ adaptive laser resonator», in *Conference on Laser and Electro-optics*, OSA Technical Digest (Optical Society of America, Washington DC, 2000), CMJ 7, p. 54]).
3. The search for the most appropriate nonlinear medium that can be used in the formation of the dynamical nonlinear mirror should be continued. This medium must have a great nonlinear coefficient and must be able to work with optical beams with high average power. The NLC cell with a thin nonlinear layer appears to be attractive for the cw self-starting laser.

The theoretical investigation should be continued in the following ways:

1. The study of the transverse mode formation in the cavity with the dynamical nonlinear mirror with the aim to increase the volume of generated mode with good quality and high average power.
2. The study of stability of generated mode in the self-starting laser.

6. Budget report

1. The total amount received from EOARD by now:	$ 35,500
2. Total Overhead of CRDF:	$ 2,931
3. Total Overhead of IAP RAS	$ 1,304
4. Total Individual Financial Support	$ 16,628
O.L. Antipov	$ 7,525
A.S. Kuzhelev	$ 3,583
D.V. Chausov	$ 1,050
A.P. Zinoviev	$ 1,000
V.A. Vorob'ev	$ 550
L.G. Kozina	$ 420
N.F. Andreev	$ 170
A.V. Fedin	$ 890
A.V. Gavrilov	$ 800
S.N. Smetanin	$ 640
5. Total equipment	$ 10,463
2 Nd:YAG rods (10×135) from «Laser Materials Corporation»	$ 4,920
1 Nd:YAG rod (6x100) from "ELS-94" Enterprise	$ 613
LiF:F saturable absorber from General Physics Institute (Moscow)	$ 500
flash-lamps ISP-5000 from "Spectr." Ent.	$ 500
the water cooling device (UO-1 type) for laser heads from "Stet" Ent.	$ 500
12x135 Nd:YAG rod purchased from "Laser Material Corp."	$ 3,430
6. Publication fee in "Optics Express" and OSA membership	$ 385
7. Amount of money for reserve by now	$ 3,789